Two-size Irregular Square Tiling Method for Isotropic Phased Array Design

P. Rocca, N. Anselmi, A. Polo, and A. Massa

Contents

Part I

Numerical Assessment

1 Irregular Phased Array Square $(1 \times 1, 2 \times 2)$-Tiling

1.1 Antenna Aperture: Rectangle 5×8 Elements

1.1.1 NON-ISOPHORIC EXCITATIONS

Exhaustive Tiling Method: ($m \times m$, $2m \times 2m$)-BMTM

Array Analysis Parameters:

- Total Number of Elements: $J = 40$;
- Spacing: $d = \lambda/2$;
- Number of Samples along u: 256;
- Number of Samples along v: 256;
- Steering Direction: $(\theta_s, \phi_s) = \{(0°, 0°)\}$;
- Tapering: CP - Symmetric Mask;
- Main Lobe Window Width along u: $MW_u = 0.7$ [u];
- Main Lobe Window Width along v: $MW_v = 1.10$ [v];
- Side Lobe levels: $SLL_1 = -30$ [dB];

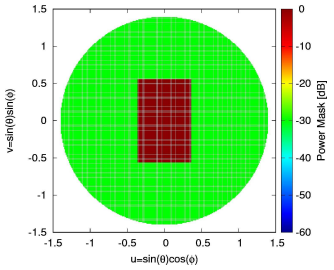

Figure 1: The power pattern mask used for the reference tapering optimization with CP.

Tiling Parameters:

- *Small* Tile: S_1-tile: 1×1;
- *Big* Tile: S_2-tile: 2×2;

- Clustering Ratio S_1-tile: $1:1$;
- Clustering Ratio S_2-tile: $1:4$;
- Total Number of Configurations: $\Gamma = 16334$;

NUMERICAL RESULTS

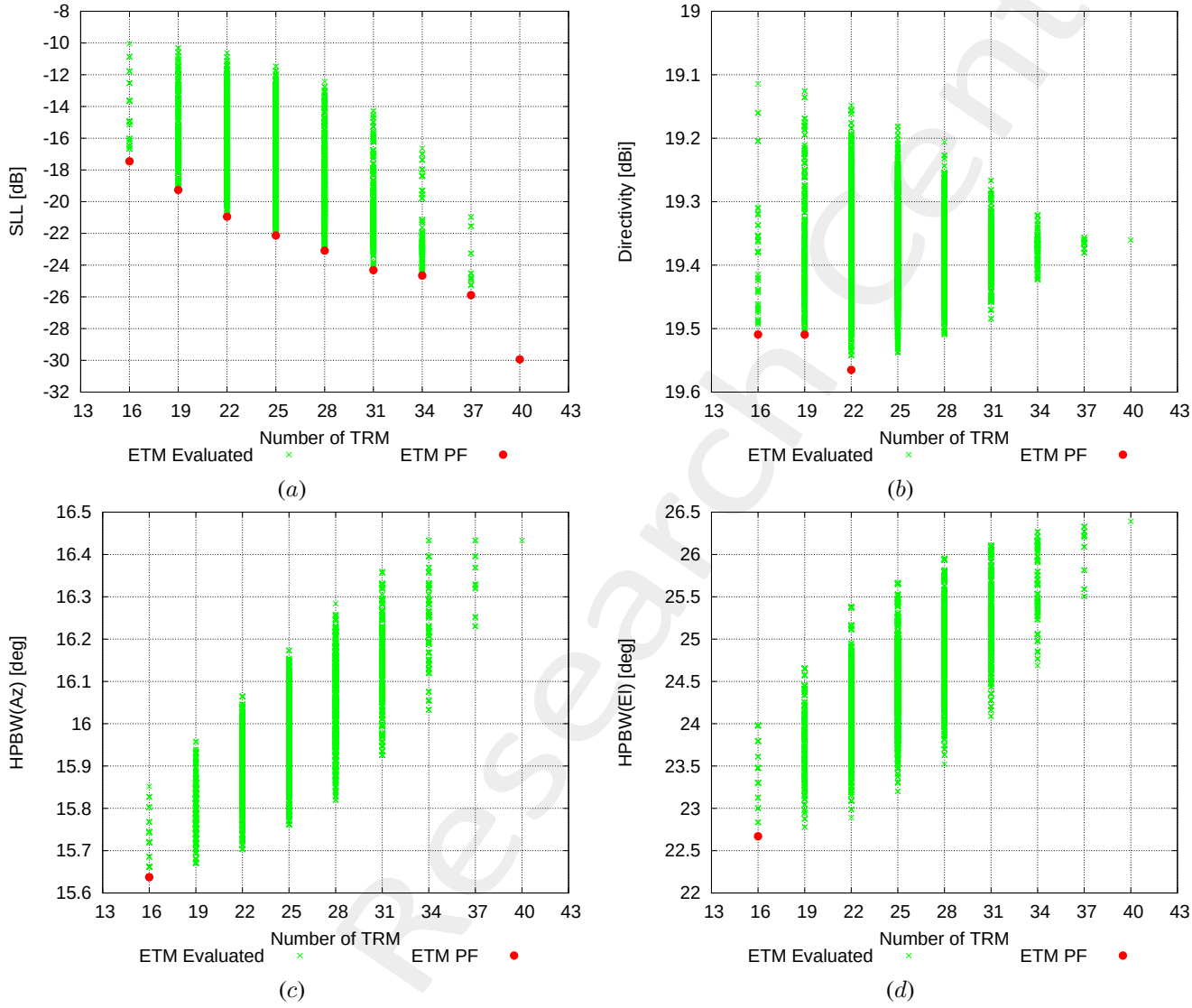

Figure 2: Numerical Assessment ($d_x = d_y = 0.5\,[\lambda]$, $k = 5$, $q = 8$, $J = 40$) - SLL vs. Number of TRM (a), $Directivity$ vs. Number of TRM (b), $HPBW(Az)$ vs. Number of TRM (c) and $HPBW(El)$ vs. Number of TRM (d).

Statistics

	Max	Min	Mean	Variance
$SLL\ [dB]$	-10.03	-29.93	-18.08	6.33
$D\ [dBi]$	19.56	19.11	19.38	3.48×10^{-3}
$HPBW_{az}\ [deg]$	16.43	15.63	15.97	1.64×10^{-2}
$HPBW_{el}\ [deg]$	26.39	22.67	24.57	0.35

Table I: Run Statistics

Number of TRM: 28

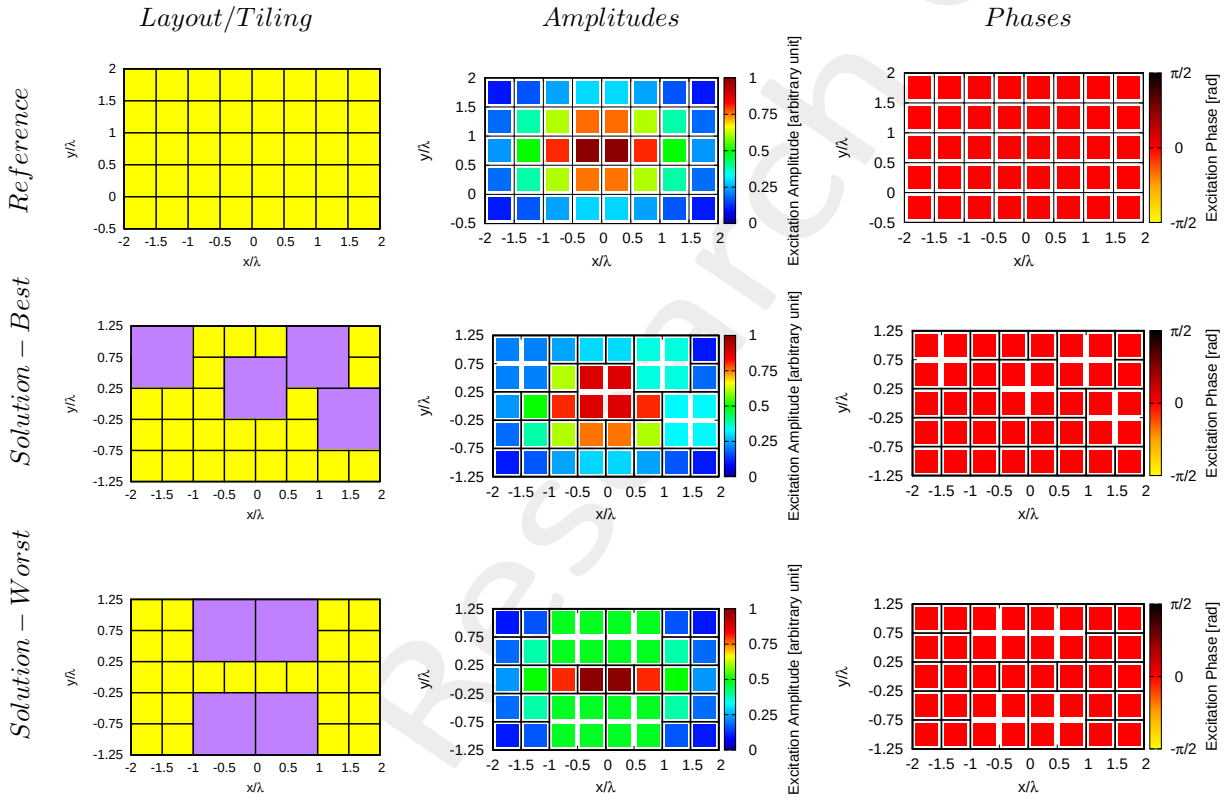

Figure 3: Numerical Assessment ($d_x = d_y = 0.5$ [λ], $k = 5$, $q = 8$, $J = 40$) - Tiling configuration and weights coefficients value.

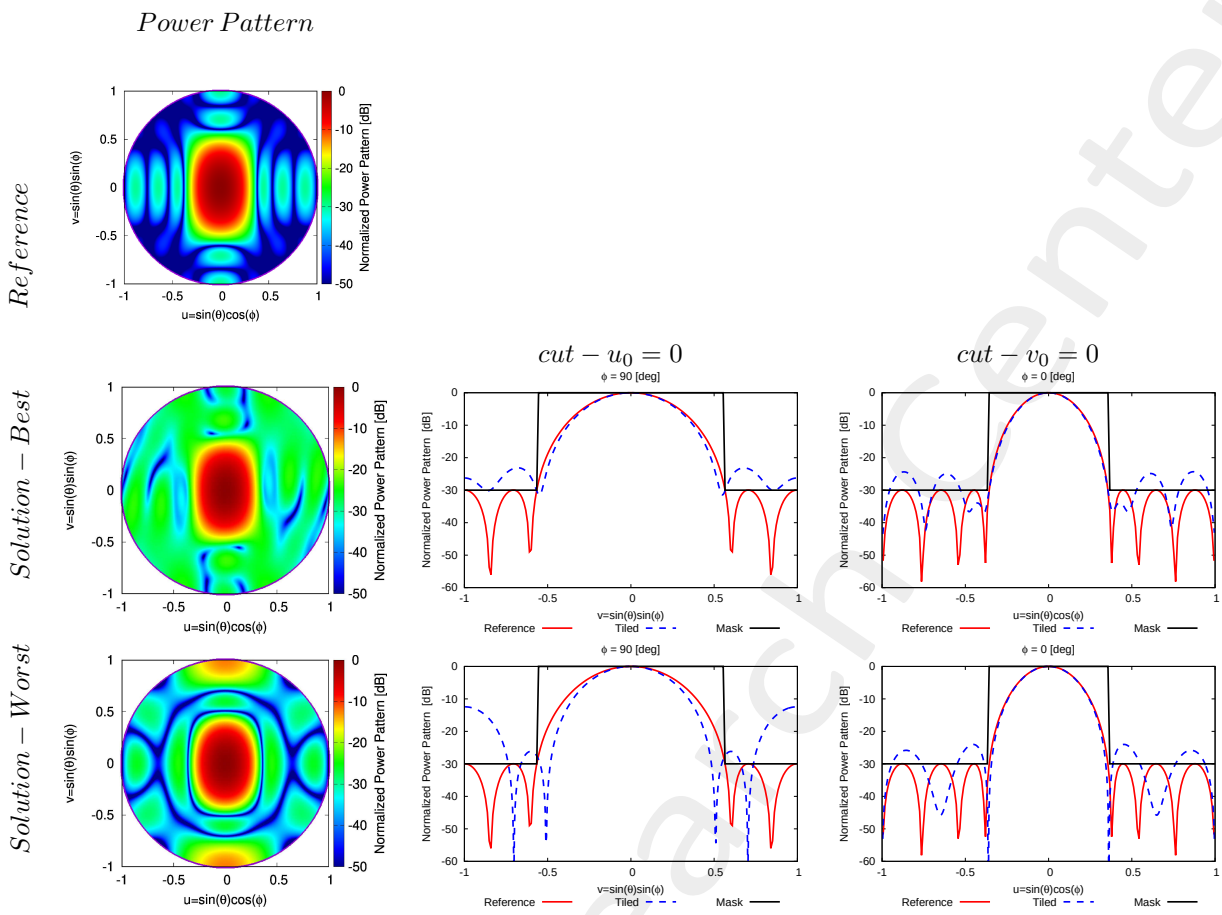

Figure 4: Numerical Assessment ($d_x = d_y = 0.5$ [λ], $k = 5$, $q = 8$, $J = 40$) - Power patterns of the solutions.

	SLL [dB]	D [dBi]	$HPBW_{az}$ [deg]	$HPBW_{el}$ [deg]
$Reference$	-29.93	$19,36$	16.43	26.39
$Solution - Best$	-23.08	19.40	16.02	25.31
$Solution - Worst$	-12.42	19.20	16.28	23.52

Table II: Pattern descriptors for the presented solutions.

Number of TRM: 19

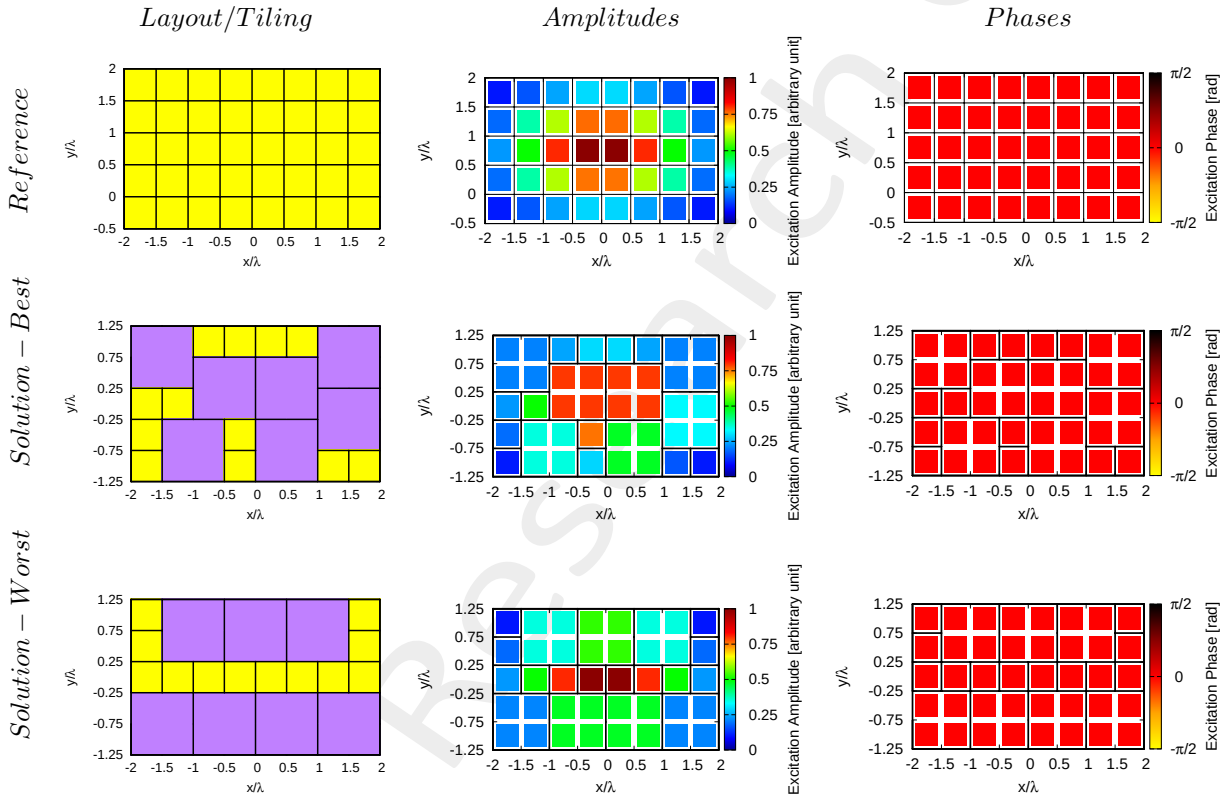

Figure 5: Numerical Assessment ($d_x = d_y = 0.5$ [λ], $k = 5$, $q = 8$, $J = 40$) - Tiling configuration and weights coefficients value.

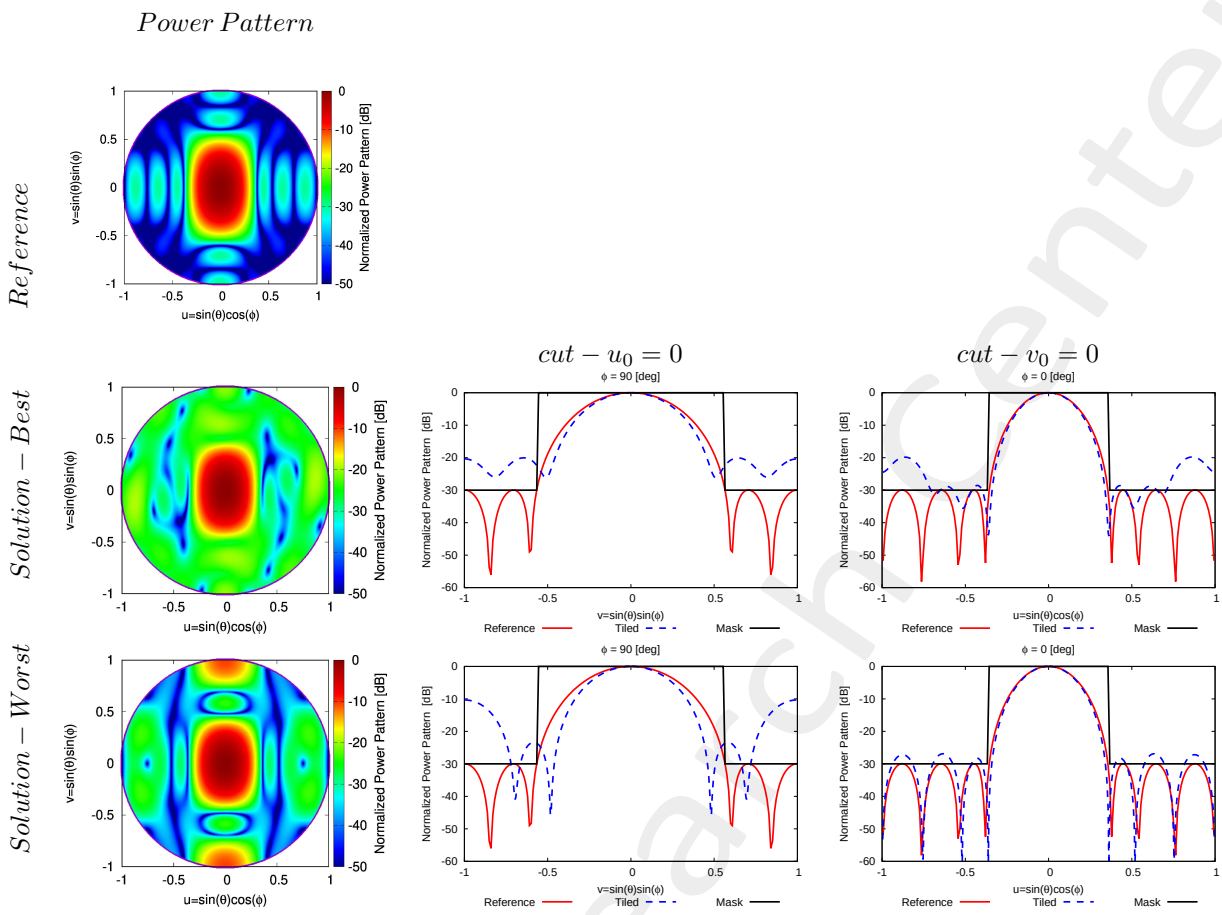

Figure 6: Numerical Assessment ($d_x = d_y = 0.5$ [λ], $k = 5$, $q = 8$, $J = 40$) - Power patterns of the solutions.

	SLL [dB]	D [dBi]	$HPBW_{az}$ [deg]	$HPBW_{el}$ [deg]
$Reference$	-29.93	$19,36$	16.43	26.39
$Solution - Best$	-19.26	19.44	15.76	24.22
$Solution - Worst$	-10.32	19.12	15.93	22.77

Table III: Pattern descriptors for the presented solutions.

Optimization-based Tiling Method: ($m \times m, 2m \times 2m$)-BMTM Integer GA

Array Analysis Parameters:

- Total Number of Elements: $J = 40$;
- Spacing: $d = \lambda/2$;
- Number of Samples along u: 256;
- Number of Samples along v: 256;
- Steering Direction: $(\theta_s, \phi_s) = \{(0°, 0°)\}$;
- Tapering: CP - Symmetric Mask;
- Main Lobe Window Width along u: $MW_u = 0.7$ [u];
- Main Lobe Window Width along v: $MW_v = 1.10$ [v];
- Side Lobe levels: $SLL_1 = -30$ [dB];

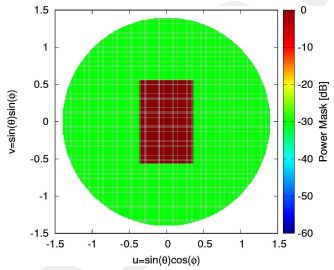

Figure 7: The power pattern mask used for the reference tapering optimization with CP.

Tiling Parameters:

- *Small* Tile: S_1-tile: 1×1;
- *Big* Tile: S_2-tile: 2×2;
- Clustering Ratio S_1-tile: $1:1$;
- Clustering Ratio S_2-tile: $1:4$;
- Total Number of Configurations: $\Gamma = 16334$;

GA Parameters:

- GA type: *Integer Genetic Algorithm;*
- Population size: $P = 10$;
- Crossover probability: $p_{CR} = 0.9$;
- Mutation probability: $p_M = 0.1$;
- Chromosome length: $l = 4$;
- Maximum number of generations: $K = 82$;
- Maximum number of allowed TRM: $TRM = 28$;
- Maximum number of functional evaluation calls: $NFE = P \times K = 820$;
- Number of initial Populations: $N_{pop} = 5$;
- Number of GA random Seeds: $N_{Seed} = 18$;
- Total number of Runs: $N_{Runs} = N_{pop} \times N_{Seed} = 90$;

NUMERICAL RESULTS

Number of TRM: 28

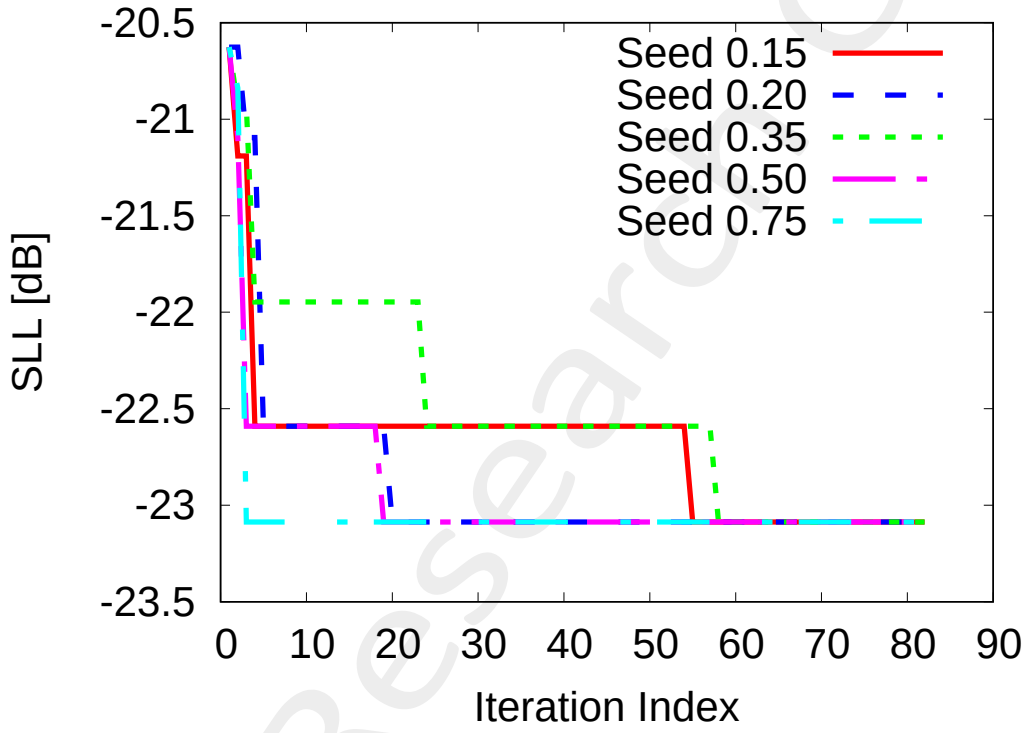

Figure 8: Numerical Assessment ($d_x = d_y = 0.5$ [λ], $k = 5$, $q = 8$, $J = 40$) - SLL vs. Iterations.

Statistics

	Max	Min	Mean	Variance
SLL [dB]	-19.60	-23.08	-22.31	0.40

Table IV: Runs Statistics

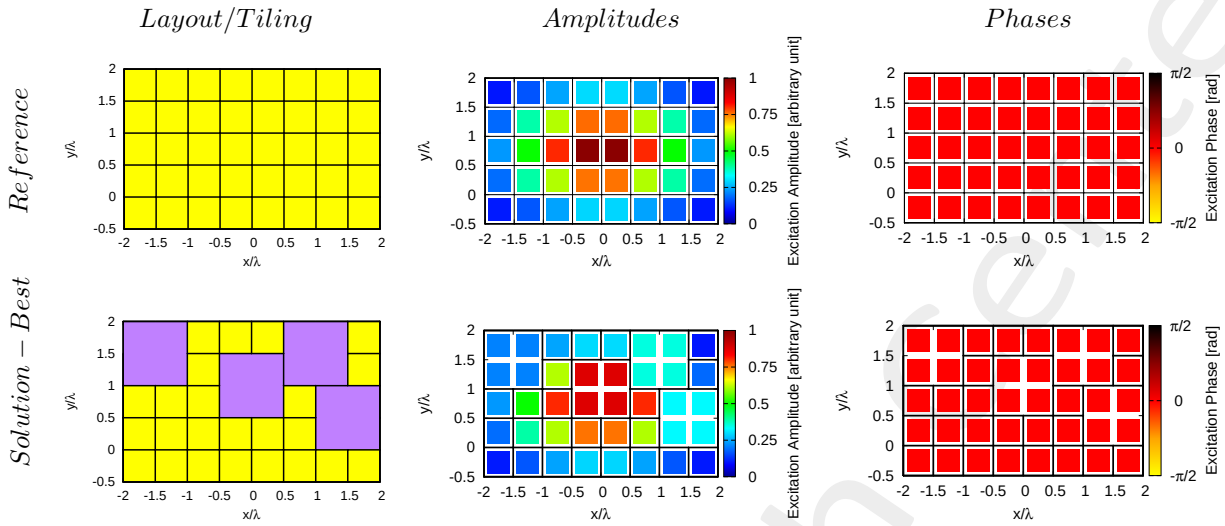

Figure 9: Numerical Assessment ($d_x = d_y = 0.5$ [λ], $k = 5$, $q = 8$, $J = 40$) - Tiling configuration and weights coefficients value.

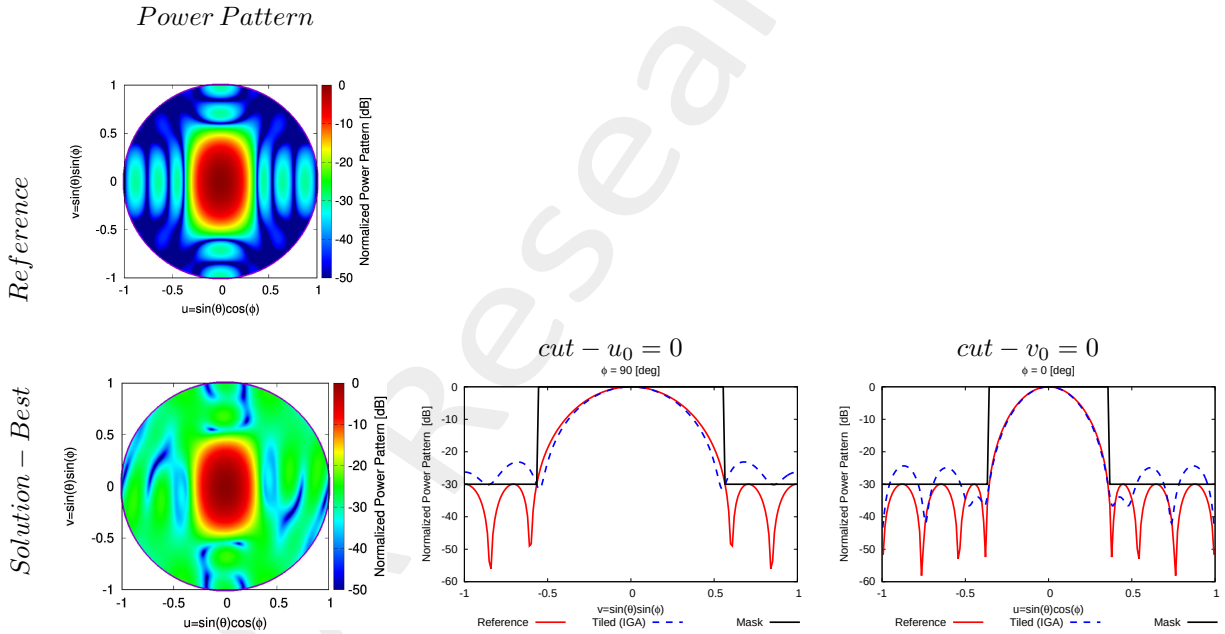

Figure 10: Numerical Assessment ($d_x = d_y = 0.5$ [λ], $k = 5$, $q = 8$, $J = 40$) - Power patterns of the solutions.

	SLL [dB]	D [dBi]	$HPBW_{az}$ [deg]	$HPBW_{el}$ [deg]
$Reference$	-29.93	$19,36$	16.43	26.39
$ETM - Best$	-23.08	19.40	16.02	25.31
$Solution - Best$	-23.08	$19,40$	16.01	25.31

Table V: Pattern descriptors for the presented solutions.

Multi-Objective Optimization-based Tiling Method: ($m \times m, 2m \times 2m$)-BMTM NSGA-III

Array Analysis Parameters:

- Total Number of Elements: $J = 40$;
- Spacing: $d = \lambda/2$;
- Number of Samples along u: 512;
- Number of Samples along v: 512;
- Steering Direction: $(\theta_s, \phi_s) = \{(0°, 0°)\}$;
- Tapering: CP - Symmetric Mask;
- Main Lobe Window Width along u: $MW_u = 0.7$ [u];
- Main Lobe Window Width along v: $MW_v = 1.10$ [v];
- Side Lobe levels: $SLL_1 = -30$ [dB];

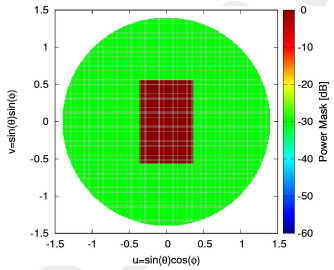

Figure 11: The power pattern mask used for the reference tapering optimization with CP.

Tiling Parameters:

- *Small* Tile: S_1-tile: 1×1;
- *Big* Tile: S_2-tile: 2×2;
- Clustering Ratio S_1-tile: $1:1$;
- Clustering Ratio S_2-tile: $1:4$;
- Total Number of Configurations: $\Gamma = 16334$;

NSGA-III Parameters:

- Population size: $P = 10$;
- Chromosome length: $l = 4$;
- Maximum number of generations: $K = 82$;
- Maximum number of functional evaluation calls: $NFE = P \times K = 820$;
- Objectives:
    1. Side-lobe Level: SLL [dB];
    2. Number of TRM: TRM;
- Number of initial Populations: $N_{pop} = 5$;
- Number of GA random Seeds: $N_{Seed} = 5$;
- Total number of Runs: $N_{Runs} = N_{pop} \times N_{Seed} = 25$;

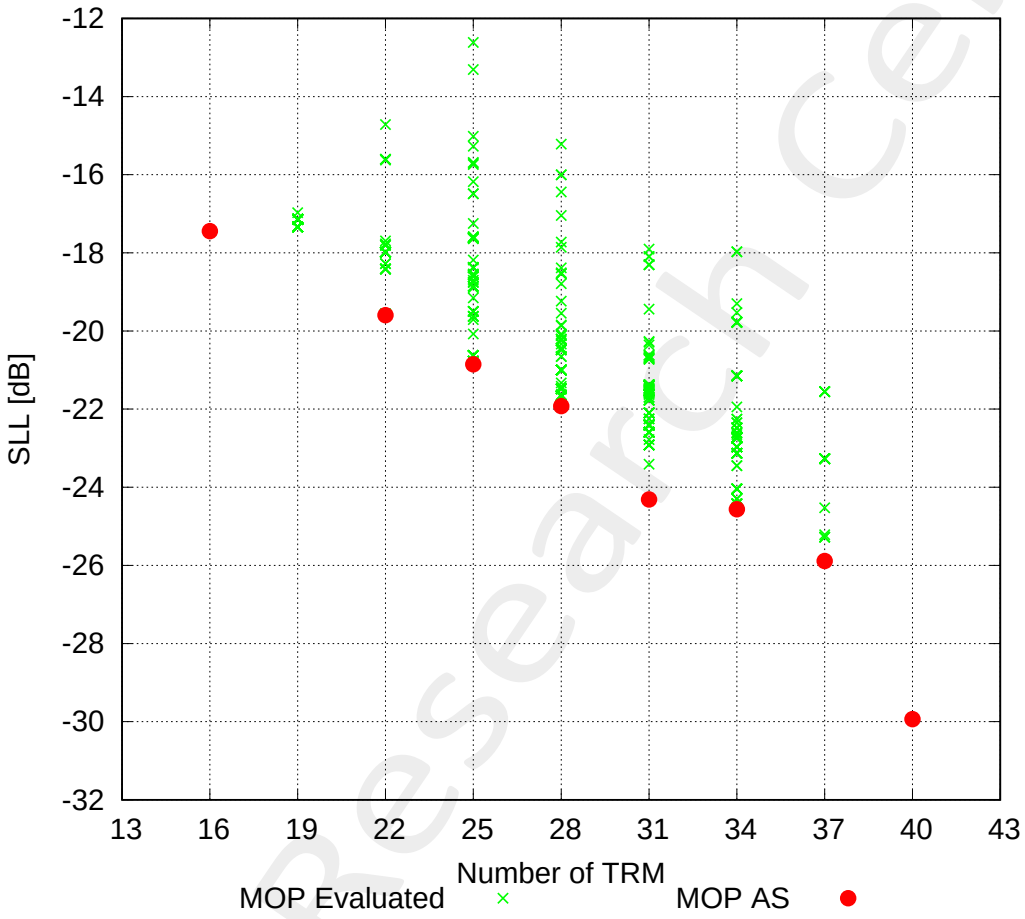

Figure 12: Numerical Assessment ($d_x = d_y = 0.5$ [λ], $k = 5$, $q = 8$, $J = 40$) - Approximation Set: Objective 1 (SLL) vs. Objective 2 (Number of TRM).

Statistics

	Max	Min	Mean	Variance
SLL [dB]	-12.60	-29.93	-20.40	5.21

Table VI: Runs Statistics

Number of TRM=40

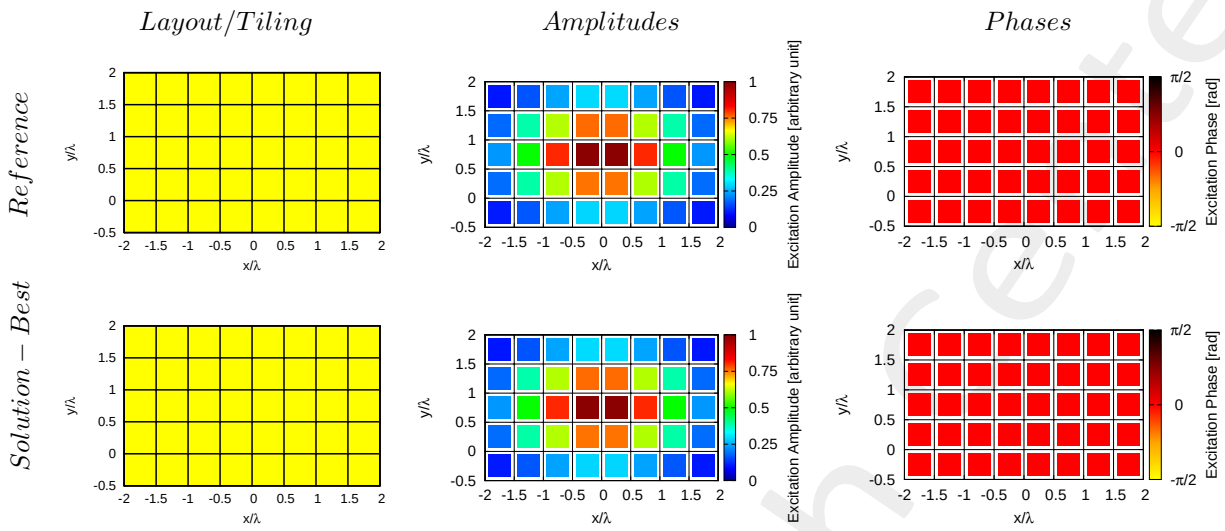

Figure 13: Numerical Assessment ($d_x = d_y = 0.5$ [λ], $k = 5$, $q = 8$, $J = 40$) - Tiling configuration and weights coefficients value.

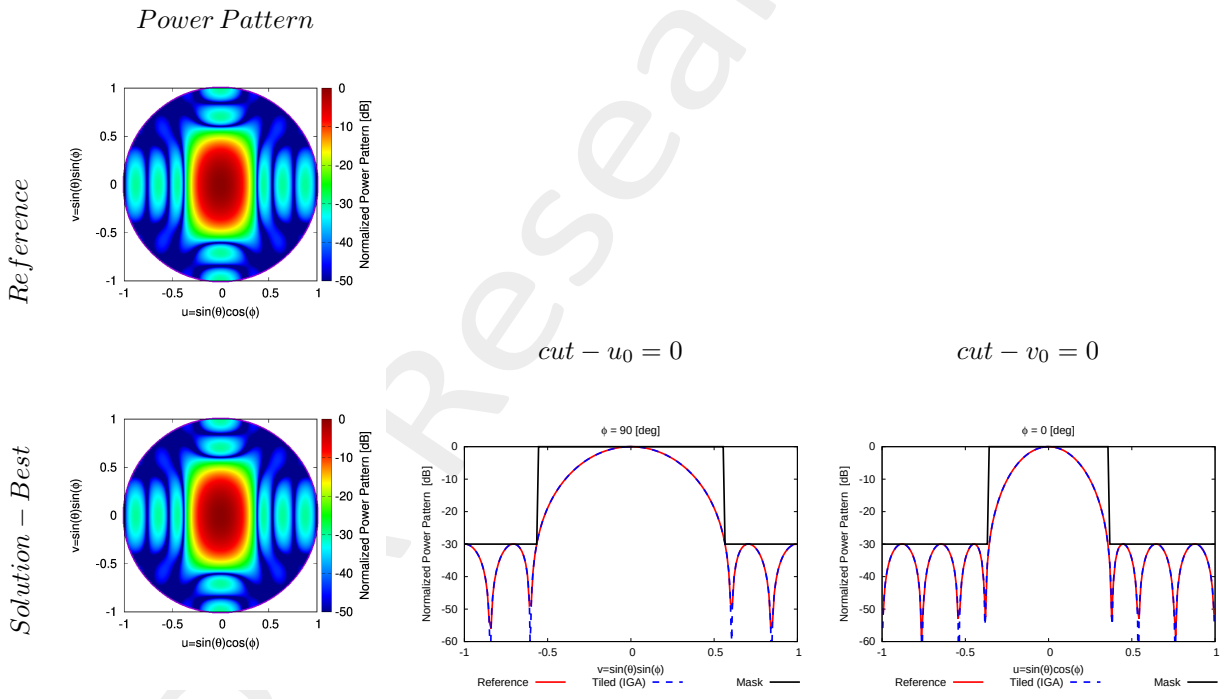

Figure 14: Numerical Assessment ($d_x = d_y = 0.5$ [λ], $k = 5$, $q = 8$, $J = 40$) - Power patterns of the solutions.

	SLL [dB]	D [dBi]	$HPBW_{az}$ [deg]	$HPBW_{el}$ [deg]
$Reference$	-29.93	$19,36$	16.43	26.39
$Solution - Best$	-29.93	$19,36$	16.43	26.39

Table VII: Pattern descriptors for the presented solutions.

Number of TRM=28

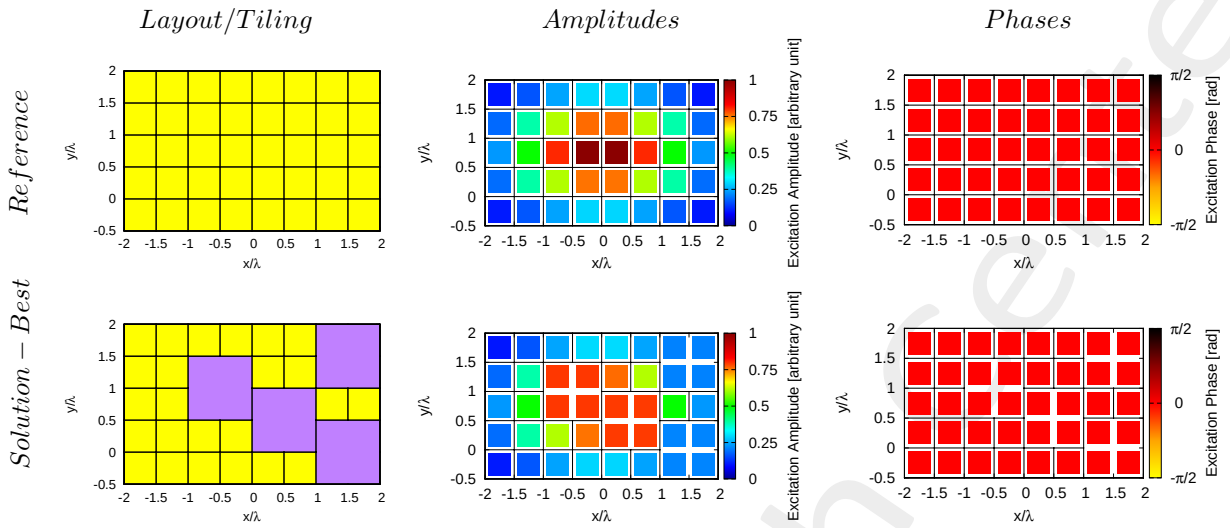

Figure 15: Numerical Assessment ($d_x = d_y = 0.5$ [λ], $k = 5$, $q = 8$, $J = 40$) - Tiling configuration and weights coefficients value.

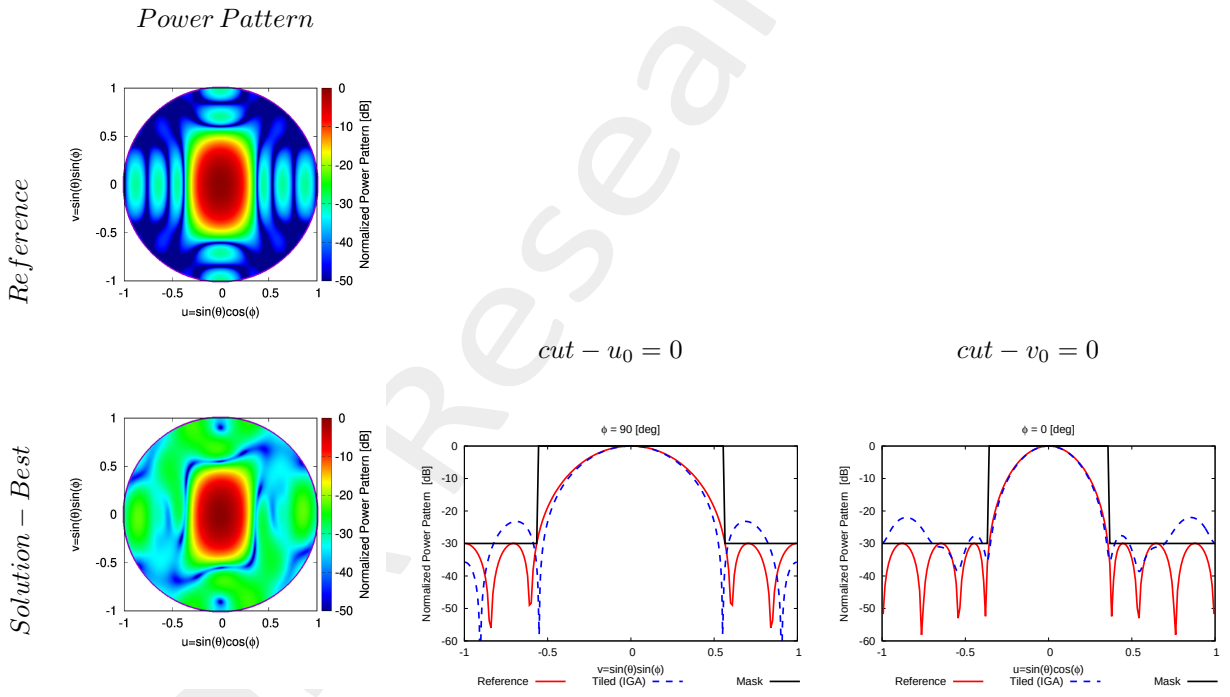

Figure 16: Numerical Assessment ($d_x = d_y = 0.5$ [λ], $k = 5$, $q = 8$, $J = 40$) - Power patterns of the solutions.

	SLL [dB]	D [dBi]	$HPBW_{az}$ [deg]	$HPBW_{el}$ [deg]
$Reference$	-29.93	$19,36$	16.43	26.39
$ETM - Best$	-23.08	19.40	16.02	25.31
$Solution - Best$	-21.92	19.36	16.08	25.48

Table VIII: Pattern descriptors for the presented solutions.

OUTCOME As can be seen from the figure below both the ETM and OTM methods have led to the same identical optimal tiling. But unlike the ETM, the OTM was able to find the optimum by exploring only a small fraction of the space of the solutions.

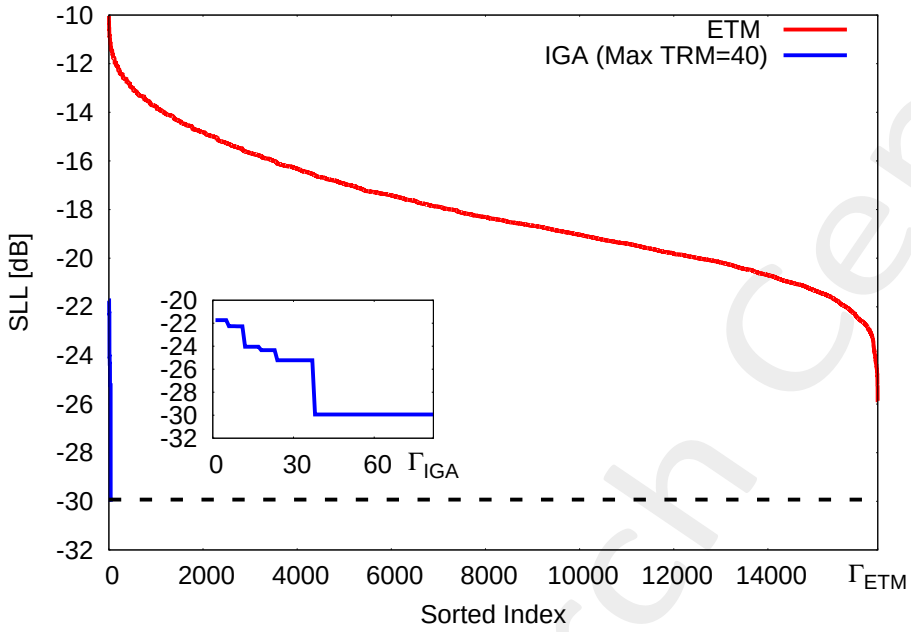

Figure 17: Numerical Assessment ($d_x = d_y = 0.5$ [λ], $k = 5$, $q = 8$, $J = 40$) - SLL vs. *Sorted Index*: ETM vs. OTM (SOP).

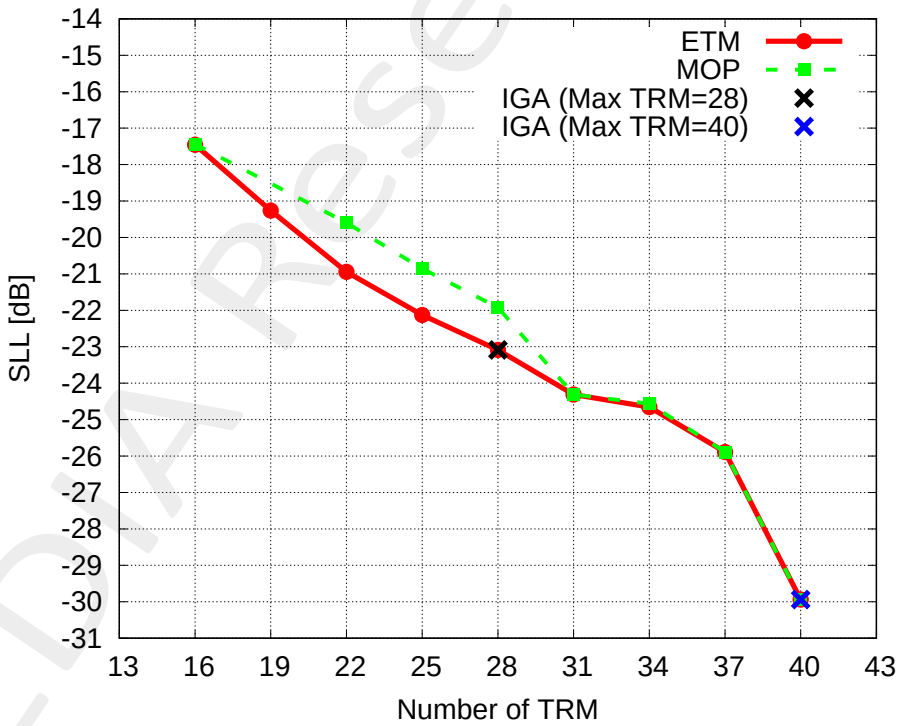

Figure 18: Numerical Assessment ($d_x = d_y = 0.5$ [λ], $k = 5$, $q = 8$, $J = 40$) - Approximation Sets (SLL vs. Number of TRM) comparison: ETM vs. OTM (SOP and MOP).

1.2 Antenna Aperture: Rectangle 10×10 Elements

1.2.1 ISOPHORIC EXCITATIONS

Optimization-based Tiling Method: $(m, 2m)$-BMTM Integer GA

Array Analysis Parameters:

- Total Number of Elements: $J = 100$;
- Spacing: $d = \lambda/2$;
- Number of Samples along u: 512;
- Number of Samples along v: 512;
- Steering Direction: $(\theta_s, \phi_s) = \{(0°, 0°)\}$;
- Tapering: Isophoric;

Tiling Parameters:

- *Small* Tile: S_1-tile: 1×1;
- *Big* Tile: S_2-tile: 2×2;
- Clustering Ratio S_1-tile: $1 : 1$;
- Clustering Ratio S_2-tile: $1 : 4$;
- Total Number of Configurations: $\Gamma = 2.69 \times 10^{11}$;

GA Parameters:

- GA type: *Integer Genetic Algorithm;*
- Population size: $P = 63$;
- Crossover probability: $p_{CR} = 0.9$:
- Mutation probability: $p_M = 0.01$;
- Chromosome length: $l = 9$;
- Maximum number of generations: $K = 30000$;
- Maximum number of functional evaluation calls: $NFE = P \times K = 18.9 \times 10^5$;
- Maximum number of allowed TRM: $TRM = 100$;
- Number of initial Populations: $N_{pop} = 5$;
- Number of GA random Seeds: $N_{Seed} = 18$;
- Total number of Runs: $N_{Runs} = N_{pop} \times N_{Seed} = 90$;

NUMERICAL RESULTS

Number of TRM: 64

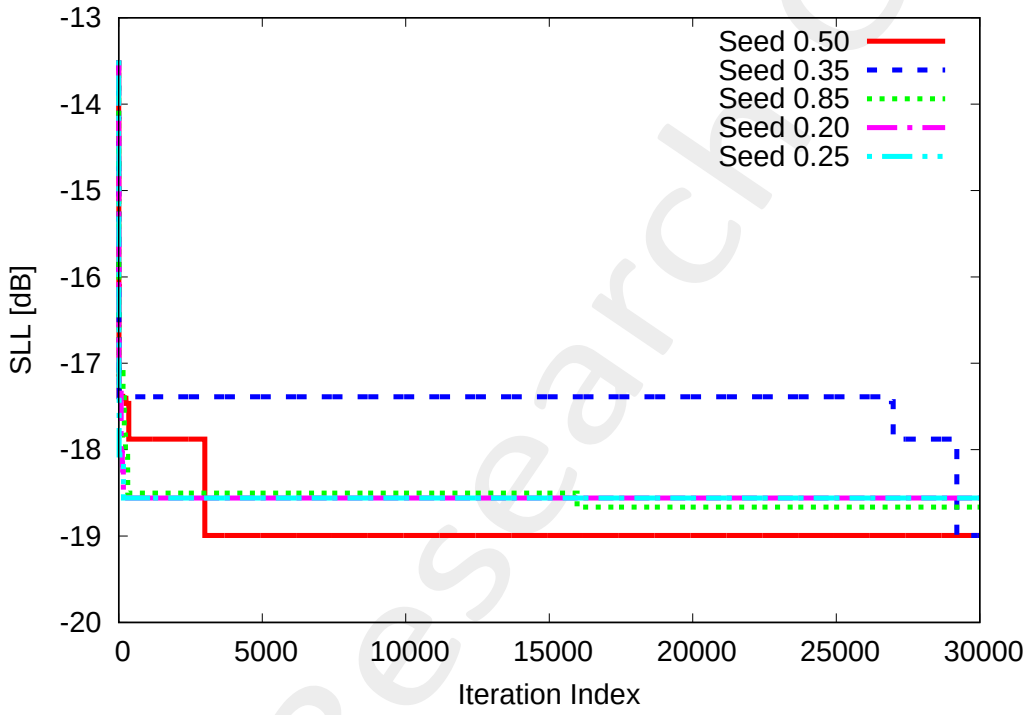

Figure 19: Numerical Assessment ($d_x = d_y = 0.5$ [λ], $k = 10$, $q = 10$, $J = 100$) - SLL vs. Iterations.

Statistics

	Max	Min	Mean	Variance
SLL [dB]	-13.49	-18.99	-18.05	0.42

Table IX: Runs Statistics

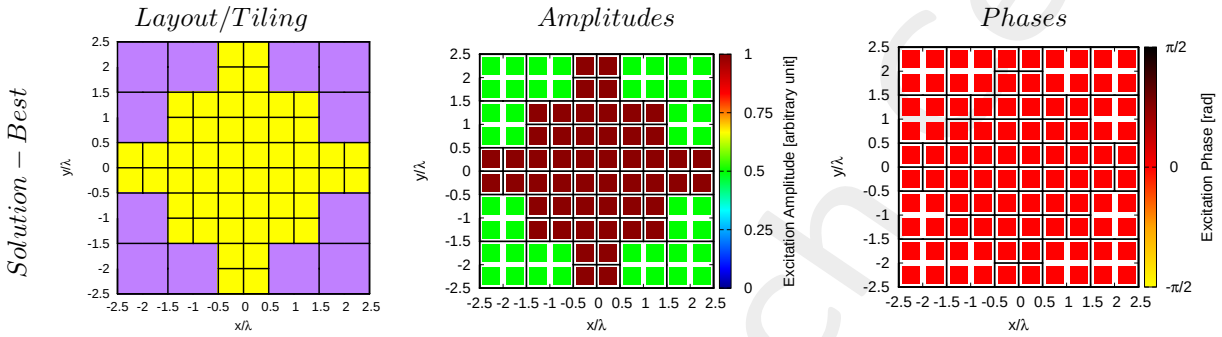

Figure 20: Numerical Assessment ($d_x = d_y = 0.5$ [λ], $k = 10$, $q = 10$, $J = 100$) - Tiling configuration and weights coefficients value.

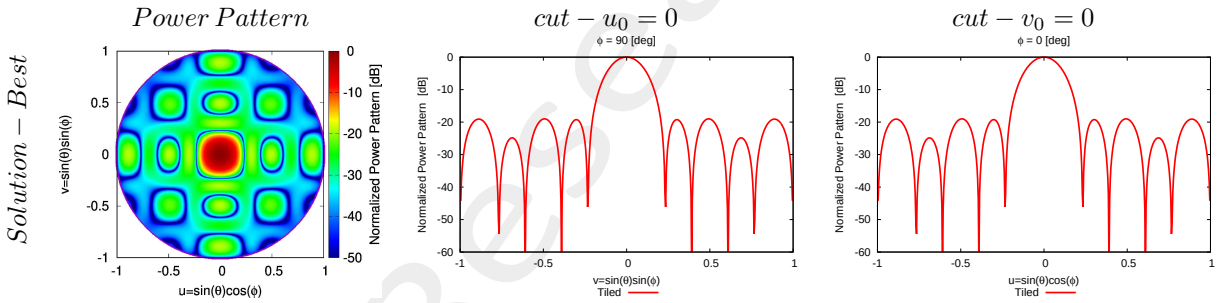

Figure 21: Numerical Assessment ($d_x = d_y = 0.5$ [λ], $k = 10$, $q = 10$, $J = 100$) - Power patterns of the solutions.

	SLL [dB]	D [dBi]	$HPBW_{az}$ [deg]	$HPBW_{el}$ [deg]
$Solution - Best$	-18.99	24.28	11.17	11.17

Table X: Pattern descriptors for the presented solutions.

Multi-Objective Optimization-based Tiling Method: ($m \times m, 2m \times 2m$)-BMTM NSGA-III

Array Analysis Parameters:

- Total Number of Elements: $J = 100$;
- Spacing: $d = \lambda/2$;
- Number of Samples along u: 512;
- Number of Samples along v: 512;
- Steering Direction: $(\theta_s, \phi_s) = \{(0°, 0°)\}$;
- Tapering: Isophoric;

Tiling Parameters:

- *Small* Tile: S_1-tile: 1×1;
- *Big* Tile: S_2-tile: 2×2;
- Clustering Ratio S_1-tile: $1 : 1$;
- Clustering Ratio S_2-tile: $1 : 4$;
- Total Number of Configurations: $\Gamma = 2.69 \times 10^{11}$;

NSGA-III Parameters:

- Population size: $P = 63$;
- Chromosome length: $l = 9$;
- Maximum number of generations: $K = 15000$;
- Maximum number of functional evaluation calls: $NFE = P \times K = 94.5 \times 10^4$;
- Objectives:
  1. Side-lobe Level: SLL [dB];
  2. Directivity: D [dBi];
  3. Number of TRM: TRM;
- Number of initial Populations: $N_{pop} = 5$.
- Number of GA random Seeds: $N_{Seed} = 5$.
- Total number of Runs: $N_{Runs} = N_{pop} \times N_{Seed} = 25$.

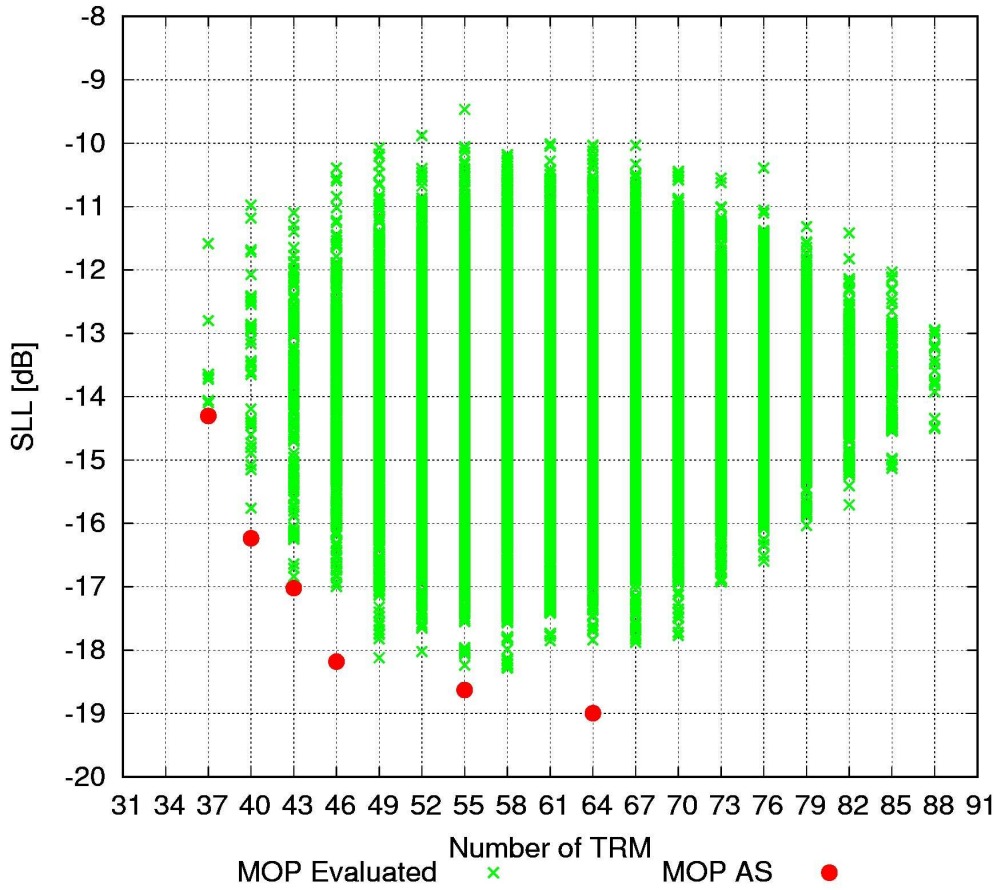

Figure 22: Numerical Assessment ($d_x = d_y = 0.5$ [λ], $k = 10$, $q = 10$, $J = 100$) - Approximation Set: Objective 1 (SLL) vs. Objective 3 (Number of TRM).

Statistics

	Max	Min	Mean	Variance
SLL [dB]	-9.46	-18.99	-16.11	2.70
D [dBi]	24.56	23.85	24.08	3.17×10^{-2}

Table XI: Runs Statistics

Number of TRM=64

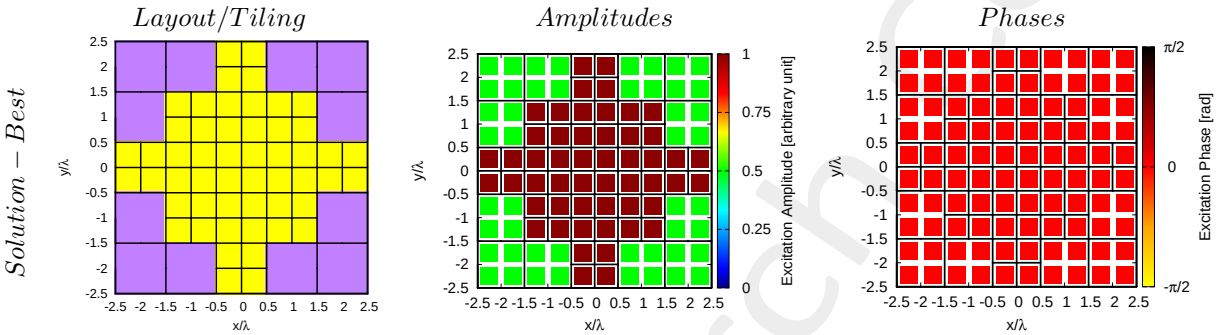

Figure 23: Numerical Assessment ($d_x = d_y = 0.5$ [λ], $k = 10$, $q = 10$, $J = 100$) - Tiling configuration and weights coefficients value.

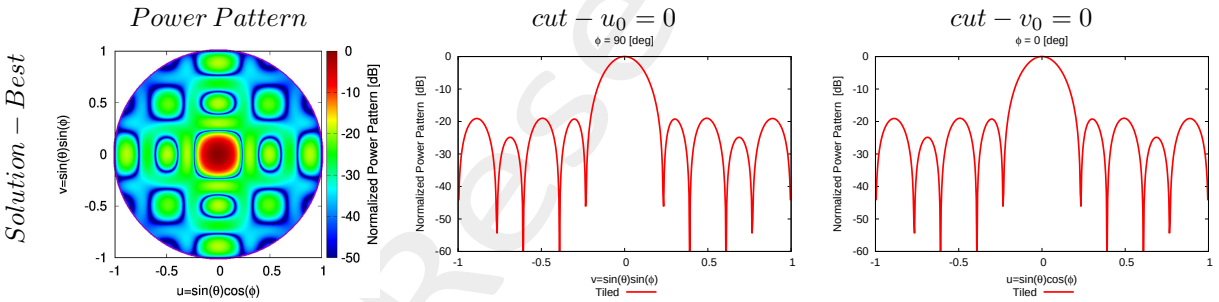

Figure 24: Numerical Assessment ($d_x = d_y = 0.5$ [λ], $k = 10$, $q = 10$, $J = 100$) - Power patterns of the solutions.

	SLL [dB]	D [dBi]	$HPBW_{az}$ [deg]	$HPBW_{el}$ [deg]
$Solution - Best$	-18.99	24.28	11.17	11.17

Table XII: Pattern descriptors for the presented solutions.

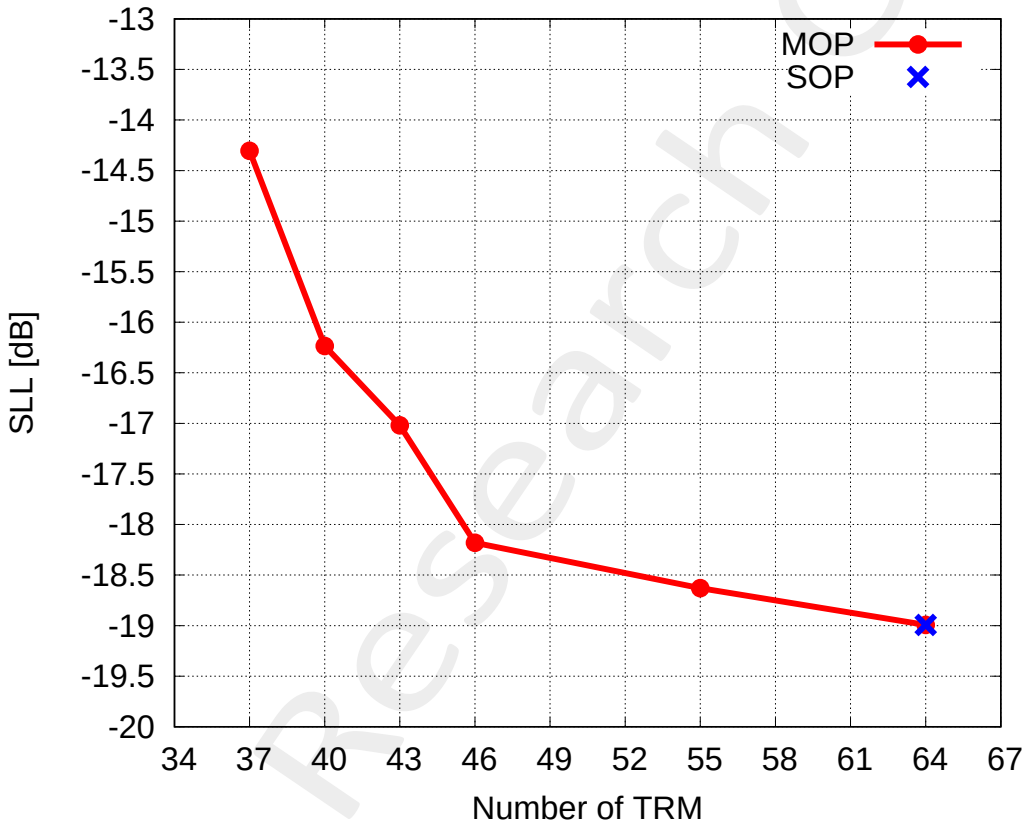

Figure 25: Numerical Assessment ($d_x = d_y = 0.5$ [λ], $k = 10$, $q = 10$, $J = 100$) - SLL vs. Number of TRM: SOP vs. MOP.

2 Irregular Phased Array Square ($1 \times 1, 4 \times 4$)-Tiling

2.1 Antenna Aperture: Rectangle 50×30 Elements

2.1.1 ISOPHORIC EXCITATIONS

Optimization-based Tiling Method: ($m \times m, 2m \times 2m$)-BMTM Integer GA

Array Analysis Parameters:

- Total Number of Elements: $J = 1500$;
- Spacing: $d = \lambda/2$;
- Number of Samples along u: 512;
- Number of Samples along v: 512;
- Steering Direction: $(\theta_s, \phi_s) = \{(0°, 0°)\}$;
- Tapering: Isophoric;

Tiling Parameters:

- *Small* Tile: S_1-tile: 1×1;
- *Big* Tile: S_2-tile: 2×2;
- Clustering Ratio S_1-tile: $1 : 1$;
- Clustering Ratio S_2-tile: $1 : 4$;

GA Parameters:

- GA type: *Integer Genetic Algorithm.*
- Population size: $P = 50$;
- Crossover probability: $p_{CR} = 0.9$;
- Mutation probability: $p_M = 0.1$;
- Chromosome length: $l = 47$;
- Maximum number of generations: $K = 10000$;
- Maximum number of allowed TRM: $TRM = 1500$;
- Maximum number of functional evaluation calls: $NFE = P \times K = 5.0 \times 10^5$;
- Number of initial Populations: $N_{pop} = 1$;
- Number of GA random Seeds: $N_{Seed} = 3$;
- Total number of Runs: $N_{Runs} = N_{pop} \times N_{Seed} = 3$;

NUMERICAL RESULTS

Number of TRM: 810

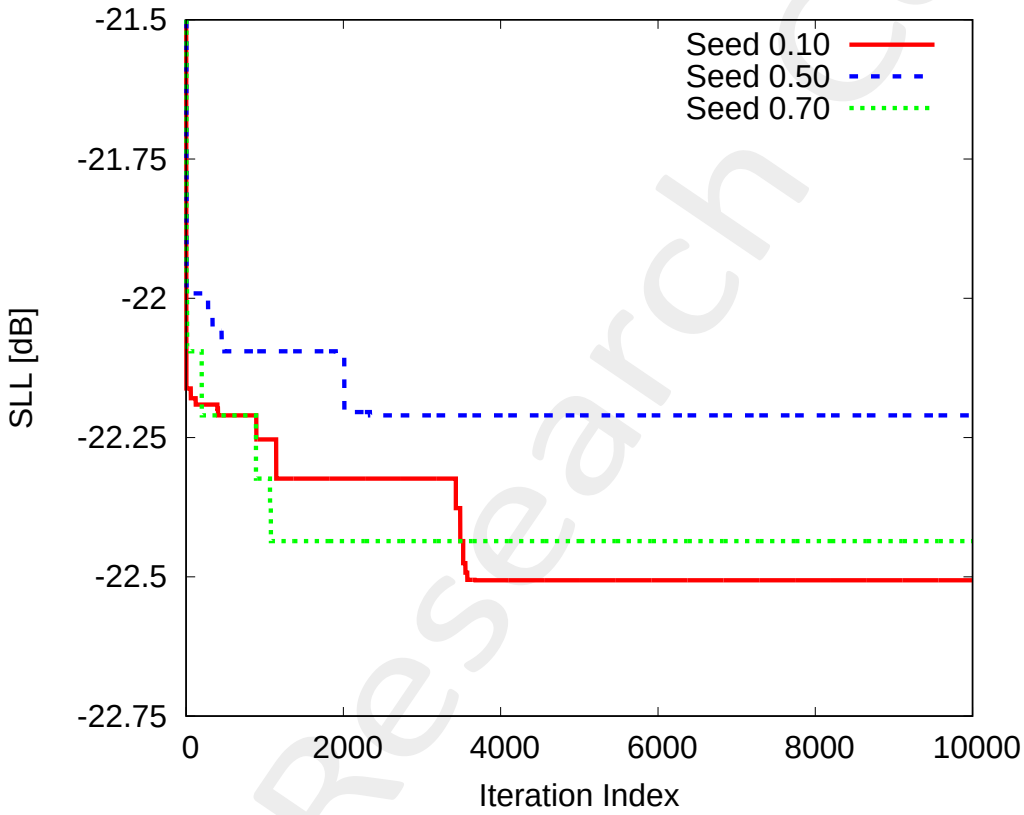

Figure 26: Numerical Assessment ($d_x = d_y = 0.5$ [λ], $k = 20$, $q = 20$, $J = 400$) - SLL vs. Iterations.

Statistics

	Max	Min	Mean	Variance
SLL [dB]	-20.89	-22.50	-22.34	1.99×10^{-2}

Table XIII: Runs Statistics

Direction ($\theta = 0°, \phi = 0°$)

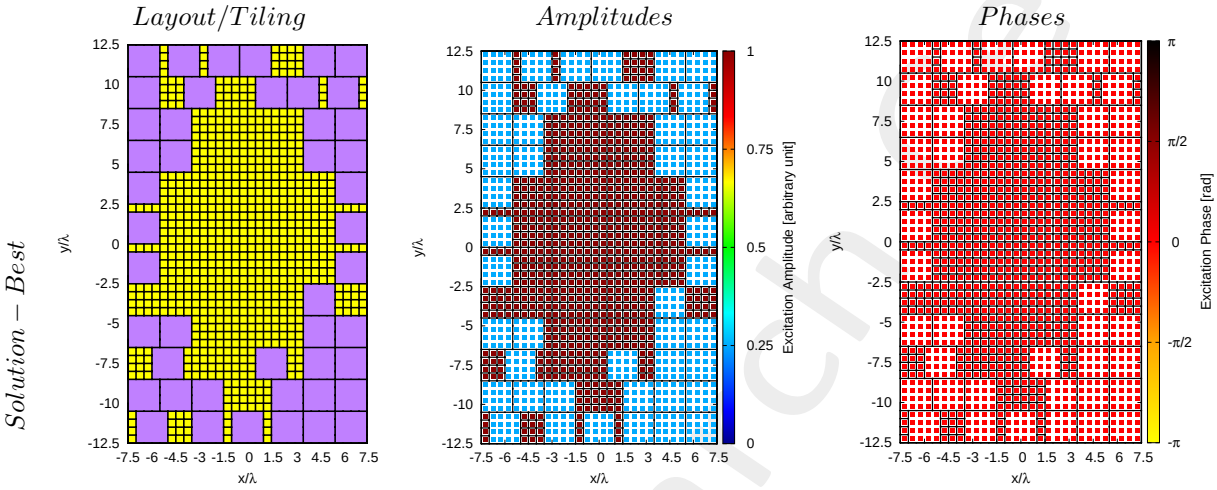

Figure 27: Numerical Assessment ($d_x = d_y = 0.5$ [λ], $k = 20$, $q = 20$, $J = 400$) - Tiling configuration and weights coefficients value.

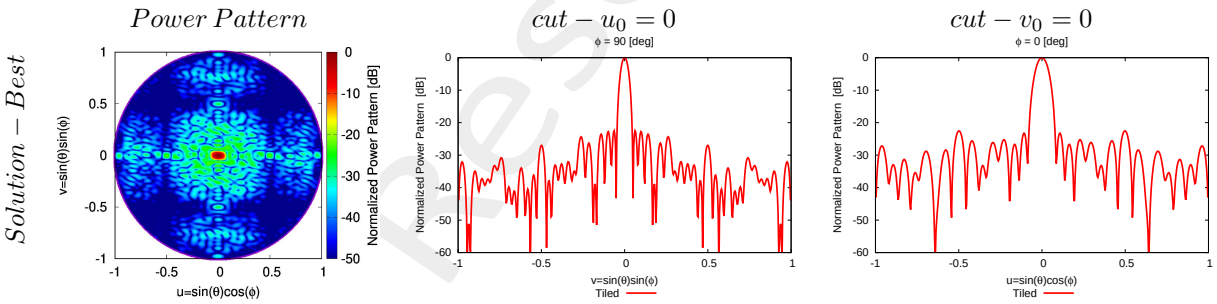

Figure 28: Numerical Assessment ($d_x = d_y = 0.5$ [λ], $k = 20$, $q = 20$, $J = 400$) - Power patterns of the solutions.

	SLL [dB]	D [dBi]	$HPBW_{az}$ [deg]	$HPBW_{el}$ [deg]
$Solution - Best$	-22.50	35.25	3.95	2.33

Table XIV: Pattern descriptors for the presented solutions.

Direction ($\theta = 5°, \phi = 0°$)

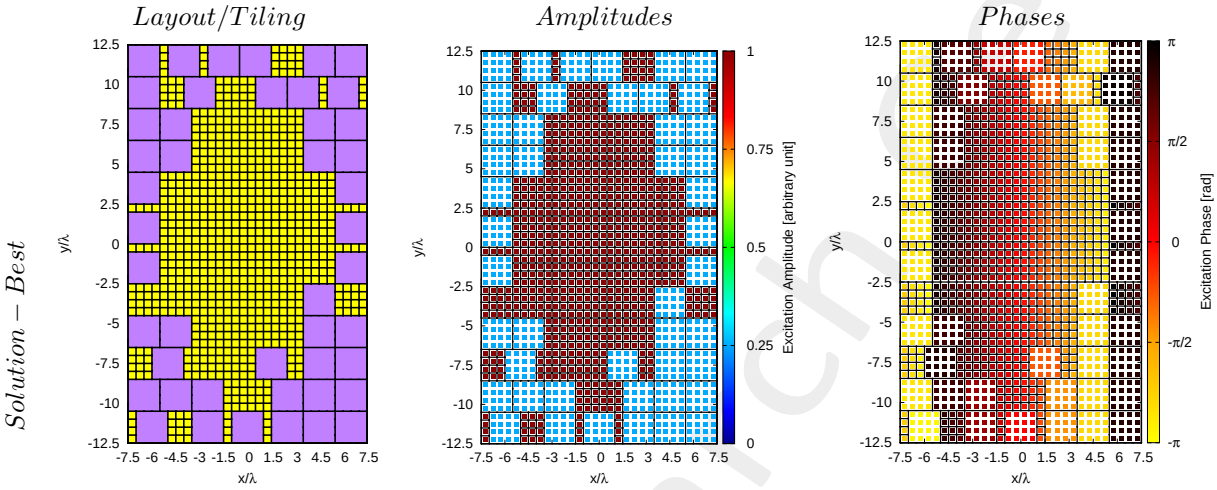

Figure 29: Numerical Assessment ($d_x = d_y = 0.5$ [λ], $k = 20$, $q = 20$, $J = 400$) - Tiling configuration and weights coefficients value.

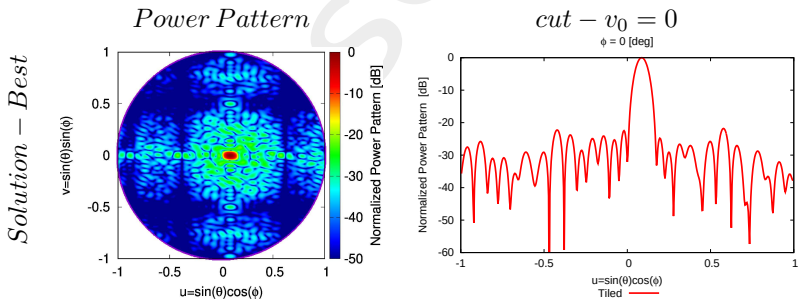

Figure 30: Numerical Assessment ($d_x = d_y = 0.5$ [λ], $k = 20$, $q = 20$, $J = 400$) - Power patterns of the solutions.

	SLL [dB]	D [dBi]	$HPBW_{az}$ [deg]	$HPBW_{el}$ [deg]
$Solution - Best$	-21.79	35.11	3.98	2.34

Table XV: Pattern descriptors for the presented solutions.

Direction ($\theta = 5°, \phi = 90°$)

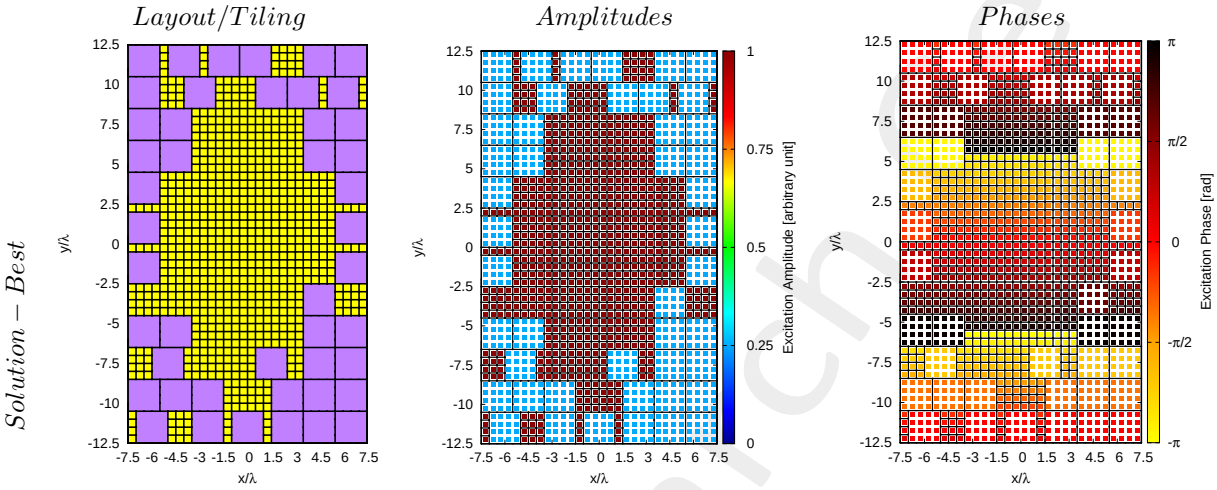

Figure 31: Numerical Assessment ($d_x = d_y = 0.5$ [λ], $k = 20$, $q = 20$, $J = 400$) - Tiling configuration and weights coefficients value.

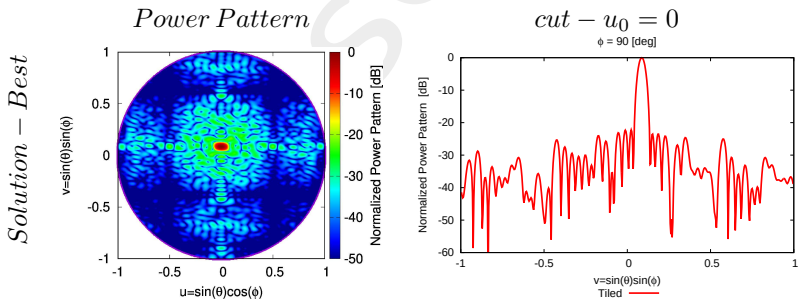

Figure 32: Numerical Assessment ($d_x = d_y = 0.5$ [λ], $k = 20$, $q = 20$, $J = 400$) - Power patterns of the solutions.

	SLL [dB]	D [dBi]	$HPBW_{az}$ [deg]	$HPBW_{el}$ [deg]
$Solution - Best$	-22.08	35.12	3.97	2.35

Table XVI: Pattern descriptors for the presented solutions.

More information on the topics of this document can be found in the following list of references.

References

[1] P. Rocca, G. Oliveri, and A. Massa, "Differential Evolution as applied to electromagnetics," *IEEE Antennas Propag. Mag.*, vol. 53, no. 1, pp. 38-49, Feb. 2011.

[2] M. Salucci, G. Gottardi, N. Anselmi, and G. Oliveri, "Planar thinned array design by hybrid analytical-stochastic optimization," *IET Microwaves, Antennas & Propagation*, vol. 11, no. 13, pp. 1841-1845, Oct. 2017

[3] P. Rocca, N. Anselmi, A. Polo, and A. Massa, "An irregular two-sizes square tiling method for the design of isophoric phased arrays," *IEEE Trans. Antennas Propag.*, vol. 68, no. 6, pp. 4437-4449, Jun. 2020.

[4] P. Rocca, N. Anselmi, A. Polo, and A. Massa, "Modular design of hexagonal phased arrays through diamond tiles," *IEEE Trans. Antennas Propag.*, vol.68, no. 5, pp. 3598-3612, May 2020.

[5] N. Anselmi, L. Poli, P. Rocca, and A. Massa, "Design of simplified array layouts for preliminary experimental testing and validation of large AESAs," *IEEE Trans. Antennas Propag.*, vol. 66, no. 12, pp. 6906-6920, Dec. 2018.

[6] N. Anselmi, P. Rocca, M. Salucci, and A. Massa, "Contiguous phase-clustering in multibeam-on-receive scanning arrays," *IEEE Trans. Antennas Propag.*, vol. 66, no. 11, pp. 5879-5891, Nov. 2018.

[7] G. Oliveri, G. Gottardi, F. Robol, A. Polo, L. Poli, M. Salucci, M. Chuan, C. Massagrande, P. Vinetti, M. Mattivi, R. Lombardi, and A. Massa, "Co-design of unconventional array architectures and antenna elements for 5G base station," *IEEE Trans. Antennas Propag.*, vol. 65, no. 12, pp. 6752-6767, Dec. 2017.

[8] N. Anselmi, P. Rocca, M. Salucci, and A. Massa, "Irregular phased array tiling by means of analytic schemata-driven optimization," *IEEE Trans. Antennas Propag.*, vol. 65, no. 9, pp. 4495-4510, September 2017.

[9] N. Anselmi, P. Rocca, M. Salucci, and A. Massa, "Optimization of excitation tolerances for robust beamforming in linear arrays," *IET Microwaves, Antennas & Propagation*, vol. 10, no. 2, pp. 208-214, 2016.

[10] P. Rocca, R. J. Mailloux, and G. Toso, "GA-Based optimization of irregular sub-array layouts for wideband phased arrays desig," *IEEE Antennas and Wireless Propag. Lett.*, vol. 14, pp. 131-134, 2015.

[11] P. Rocca, M. Donelli, G. Oliveri, F. Viani, and A. Massa, "Reconfigurable sum-difference pattern by means of parasitic elements for forward-looking monopulse radar," *IET Radar, Sonar & Navigation*, vol 7, no. 7, pp. 747-754, 2013.

[12] P. Rocca, L. Manica, and A. Massa, "Ant colony based hybrid approach for optimal compromise sum-difference patterns synthesis," *Microwave Opt. Technol. Lett.*, vol. 52, no. 1, pp. 128-132, Jan. 2010.

[13] G. Oliveri, A. Gelmini, A. Polo, N. Anselmi, and A. Massa, "System-by-design multi-scale synthesis of task-oriented reflectarrays," *IEEE Trans. Antennas Propag.*, vol. 68, no. 4, pp. 2867-2882, Apr. 2020.

[14] N. Anselmi, L. Poli, P. Rocca, and A. Massa, "Design of simplified array layouts for preliminary experimental testing and validation of large AESAs," *IEEE Trans. Antennas Propag.*, vol. 66, no. 12, pp. 6906-6920, Dec. 2018.

[15] M. Salucci, F. Robol, N. Anselmi, M. A. Hannan, P. Rocca, G. Oliveri, M. Donelli, and A. Massa, "S-Band spline-shaped aperture-stacked patch antenna for air traffic control applications," *IEEE Tran. Antennas Propag.*, vol. 66, no. 8, pp. 4292-4297, Aug. 2018.

[16] M. Salucci, L. Poli, A. F. Morabito, and P. Rocca, "Adaptive nulling through subarray switching in planar antenna arrays," *Journal of Electromagnetic Waves and Applications*, vol. 30, no. 3, pp. 404-414, February 2016

[17] T. Moriyama, L. Poli, and P. Rocca, "Adaptive nulling in thinned planar arrays through genetic algorithms," *IEICE Electronics Express*, vol. 11, no. 21, pp. 1-9, Sep. 2014.

[18] L. Poli, P. Rocca, M. Salucci, and A. Massa, "Reconfigurable thinning for the adaptive control of linear arrays," *IEEE Trans. Antennas Propag.*, vol. 61, no. 10, pp. 5068-5077, Oct. 2013.

[19] P. Rocca, L. Poli, G. Oliveri, and A. Massa, "Adaptive nulling in time-varying scenarios through time-modulated linear arrays," *IEEE Antennas Wireless Propag. Lett.*, vol. 11, pp. 101-104, 2012.

[20] P. Rocca, L. Poli, A. Polo, and A. Massa, "Optimal excitation matching strategy for sub-arrayed phased linear arrays generating arbitrary shaped beams," *IEEE Trans. Antennas Propag.*, vol. 68, no. 6, pp. 4638-4647, Jun. 2020.

[21] G. Oliveri, G. Gottardi and A. Massa, "A new meta-paradigm for the synthesis of antenna arrays for future wireless communications," *IEEE Trans. Antennas Propag.*, vol. 67, no. 6, pp. 3774-3788, Jun. 2019.

[22] P. Rocca, M. H. Hannan, L. Poli, N. Anselmi, and A. Massa, "Optimal phase-matching strategy for beam scanning of sub-arrayed phased arrays," *IEEE Trans. Antennas and Propag.*, vol. 67, no. 2, pp. 951-959, Feb. 2019.

[23] N. Anselmi, P. Rocca, M. Salucci, and A. Massa, "Contiguous phase-clustering in multibeam-on-receive scanning arrays," *IEEE Trans. Antennas Propag.*, vol. 66, no. 11, pp. 5879-5891, Nov. 2018.

[24] L. Poli, G. Oliveri, P. Rocca, M. Salucci, and A. Massa, "Long-Distance WPT Unconventional Arrays Synthesis," *Journal of Electromagnetic Waves and Applications*, vol. 31, no. 14, pp. 1399-1420, Jul. 2017.

[25] G. Gottardi, L. Poli, P. Rocca, A. Montanari, A. Aprile, and A. Massa, "Optimal Monopulse Beamforming for Side-Looking Airborne Radars," *IEEE Antennas Wireless Propag. Lett.*, vol. 16, pp. 1221-1224, 2017.

[26] G. Oliveri, M. Salucci, and A. Massa, "Synthesis of modular contiguously clustered linear arrays through a sparseness-regularized solver," *IEEE Trans. Antennas Propag.*, vol. 64, no. 10, pp. 4277-4287, Oct. 2016.

[27] P. Rocca, G. Oliveri, R. J. Mailloux, and A. Massa, "Unconventional phased array architectures and design Methodologies - A review," *Proceedings of the IEEE = Special Issue on 'Phased Array Technologies', Invited Paper*, vol. 104, no. 3, pp. 544-560, March 2016.

[28] P. Rocca, M. D'Urso, and L. Poli, "Advanced strategy for large antenna array design with subarray-only amplitude and phase contr," *IEEE Antennas and Wireless Propag. Lett.*, vol. 13, pp. 91-94, 2014.

[29] L. Manica, P. Rocca, G. Oliveri, and A. Massa, "Synthesis of multi-beam sub-arrayed antennas through an excitation matching strategy," *IEEE Trans. Antennas Propag.*, vol. 59, no. 2, pp. 482-492, Feb. 2011.

[30] G. Oliveri, "Multi-beam antenna arrays with common sub-array layouts," *IEEE Antennas Wireless Propag. Lett.*, vol. 9, pp. 1190-1193, 2010.

[31] L. T. P. Bui, N. Anselmi, T. Isernia, P. Rocca, and A. F. Morabito, "On bandwidth maximization of fixed-geometry arrays through convex programming," *Journal of Electromagnetic Waves and Applications*, vol. 34, no. 5, pp. 581-600, 2020.

[32] N. Anselmi, L. Poli, P. Rocca, and A. Massa, "Design of simplified array layouts for preliminary experimental testing and validation of large AESAs," *IEEE Trans. Antennas Propag.*, vol. 66, no. 12, pp. 6906-6920, Dec. 2018.

[33] G. Gottardi, L. Poli, P. Rocca, A. Montanari, A. Aprile, and A. Massa, "Optimal Monopulse Beamforming for Side-Looking Airborne Radars," *IEEE Antennas Wireless Propag. Lett.*, vol. 16, pp. 1221-1224, 2017.

[34] G. Oliveri and T. Moriyama, "Hybrid PS-CP technique for the synthesis of n-uniform linear arrays with maximum directivi," *Journal of Electromagnetic Waves and Applications*, vol. 29, no. 1, pp. 113-123, Jan. 2015.

[35] P. Rocca and A. Morabito, "Optimal synthesis of reconfigurable planar arrays with simplified architectures for monopulse radar applications," *IEEE Trans. Antennas Propag.*, vol. 63, no. 3, pp. 1048-1058, Mar. 2015.

[36] A. F. Morabito and P. Rocca, "Reducing the number of elements in phase-only reconfigurable arrays generating sum and difference patterns," *IEEE Antennas and Wireless Propagation Letters*, vol. 14, pp. 1338-1341, 2015.

[37] P. Rocca, N. Anselmi, and A. Massa, "Optimal synthesis of robust beamformer weights exploiting interval analysis and convex optimization," *IEEE Trans. Antennas Propag.*, vol. 62, no. 7, pp. 3603-3612, Jul. 2014.

[38] A. Morabito and P. Rocca, "Optimal synthesis of sum and difference patterns with arbitrary sidelobes subject to common excitations constraints," *IEEE Antennas Wireless Propag. Lett.*, vol. 9, pp. 623-626, 2010.

[39] D. Sartori, G. Oliveri, L. Manica, and A. Massa, "Hybrid design of no-regular linear arrays with accurate control of the pattern sidelobe," *IEEE Trans. Antennas Propag.*, vol. 61, no. 12, pp. 6237-6242, Dec. 2013.